

On-chip metal/polypyrrole quasi-reference electrodes for robust ISFET operation

Carlos Duarte-Guevara^{1,6}, Vikhram Swaminathan^{2,6}, Mark Burgess³, Bobby Reddy, Jr.⁶,

Eric Salm⁶, Yi-Shao Liu⁴, Joaquin Rodriguez-Lopez³, and Rashid Bashir^{5,6}

¹ Department of Electrical and Computer Engineering, University of Illinois at Urbana-Champaign.

² Department of Mechanical Science and Engineering, University of Illinois at Urbana-Champaign.

³ Department of Chemistry, University of Illinois at Urbana-Champaign.

⁴ Taiwan Semiconductor Manufacturing Company.

⁵ Department of Bioengineering, University of Illinois at Urbana-Champaign.

⁶ Micro and Nanotechnology Lab, University of Illinois at Urbana-Champaign.

Abstract

In this supplementary section we present figures with information that is complementary to the performed experiments. We present images that describe in greater detail the electrochemical cell used for polypyrrole deposition, present pH-dependent transfer curves of HfO₂ ISFETs, and show independent plots of the pH sensitivity obtained with different electrodes to stress differences. In addition, we show results of cyclic voltammetry deposition in other metals that are discussed in the main text. These supplementary plots show successful cyclic voltammetry (CV) deposition in palladium and iron but unsuccessful results in copper, aluminum, and titanium. For electrodes successfully coated, we show stability and pH response and for the unsuccessful ones we analyze causes and indicate possible strategies for successful polypyrrole polymerization. Finally we present CV results of electrodeposition in microelectrodes patterned on the ISFET chip and X-ray diffraction patterns of the polypyrrole coated electrodes.

Supplementary Figures

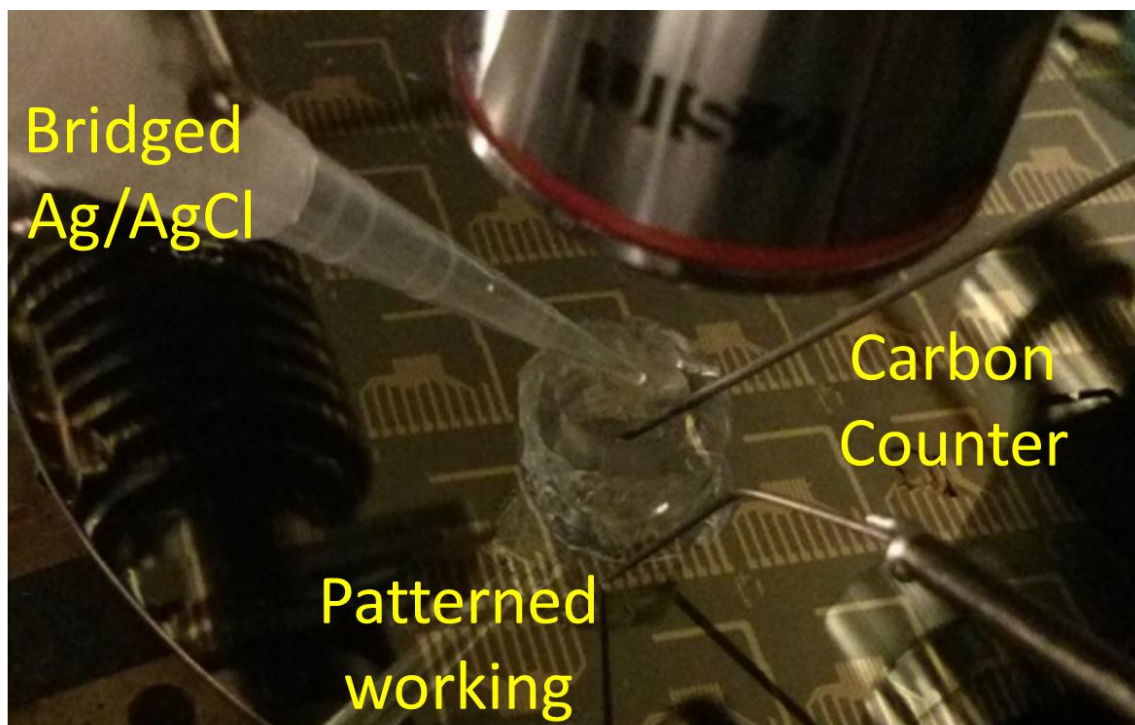


Fig. S1 Photograph of the 3 electrode cell that was used for fabrication of the on-chip polypyrrole quasi reference electrodes. The image shows the Ag/AgCl bridged with a pipette tip filled with Agar gel, the graphite counter, and a micromanipulator contacting the electrode patterned in a silicon wafer.

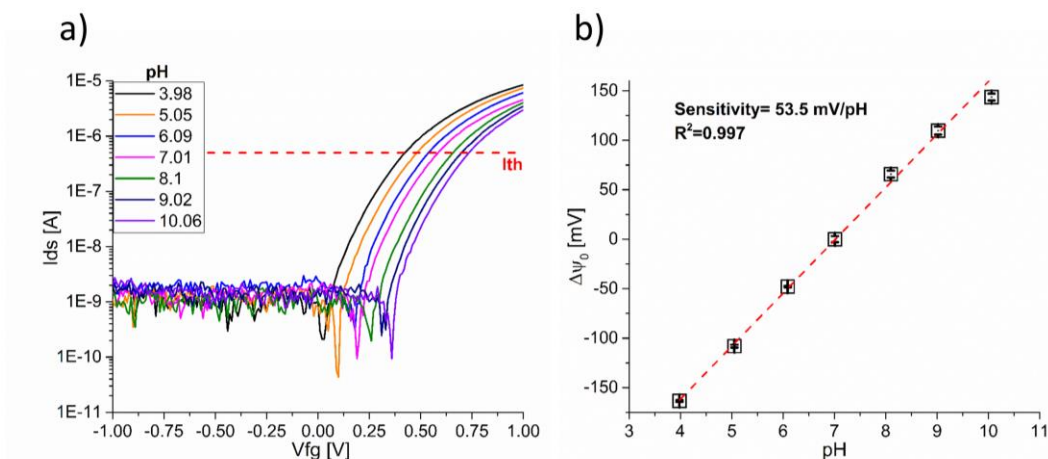


Fig. S2 pH response of hafnium oxide ISFET using a leak-free Ag/AgCl reference electrode. **(a)** Typical pH-dependent transfer curves in a range of 4 to 10. **(b)** Extracted surface potential changes as a function of pH. The slope of the linear regression is reported as sensitivity.

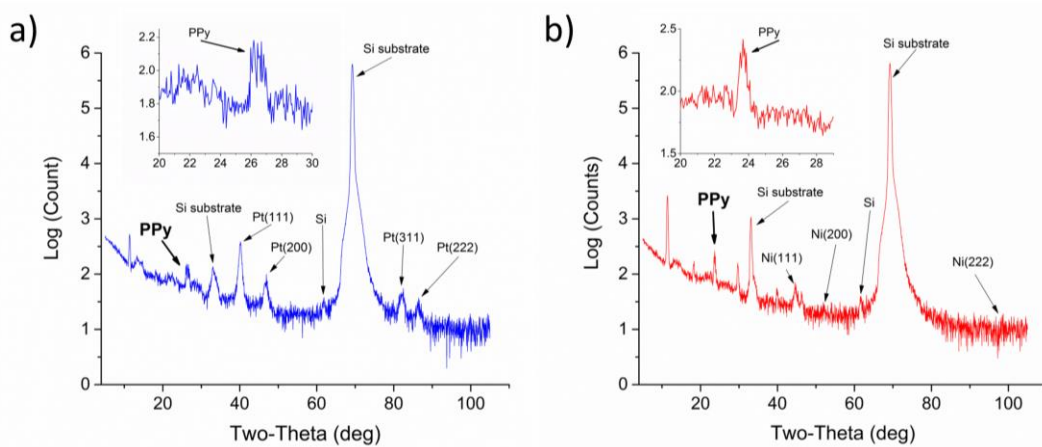


Fig. S3 X-ray diffraction pattern of the polypyrrole film deposited through the cyclic voltammetry process on **(a)** platinum and **(b)** nickel electrodes. The inset figures zoom in the region where the polypyrrole peak is observed.

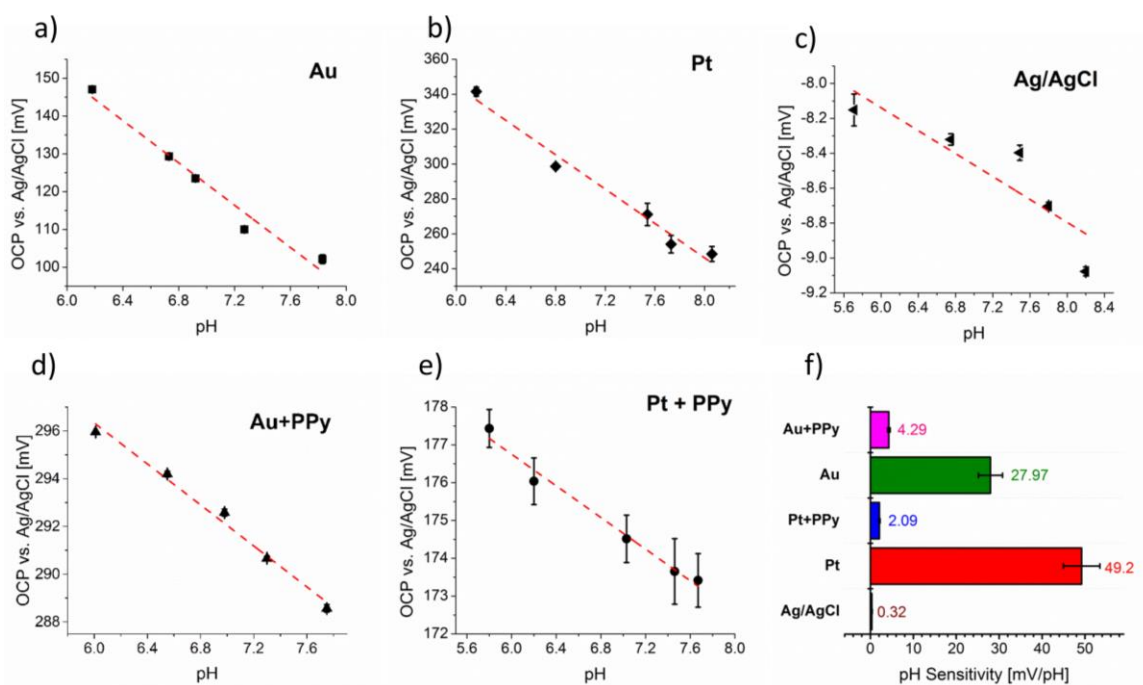


Fig. S4 pH sensitivity of on-chip electrodes with and without PPy, and a Ag/AgCl benchmark. This is the same data presented in Fig 3c of the main text but having an individual axis with a different scale for each experiment to reveal the trend of pH response. (a) Presents the behavior of gold, (b) of platinum, (c) of the Ag/AgCl reference, (d) of PPy coated gold, and (e) of coated platinum. Sensitivity data (slope of the linear regression) is summarized in (f) that was also presented in Figure 3e of the main text.

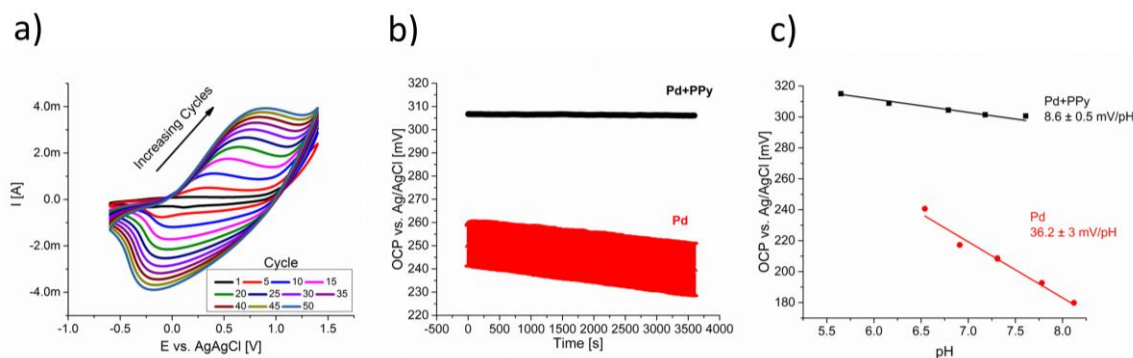


Fig. S5 Deposition on palladium microelectrodes and electrical characterization results. (a) CV deposition of PPy film on palladium microelectrodes. (b) Bands of OCP stability as a function of time for palladium with and without the PPy layer. (c) OCP vs. electrolyte pH to assess pH sensitivity of palladium and palladium+PPy electrodes. The results of the linear regressions are reported as sensitivity.

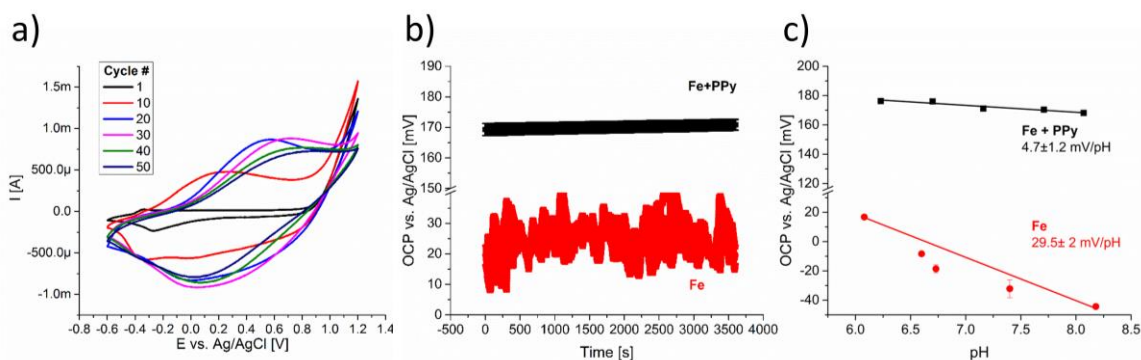


Fig. S6 Deposition on iron microelectrodes and electrical characterization results. (a) CV deposition of PPy film on iron microelectrodes. (b) Bands of OCP stability as a function of time for iron with and without the PPy layer. (c) OCP vs. electrolyte pH to assess pH sensitivity of iron and iron+PPy electrodes. The results of the linear regressions are reported as sensitivity.

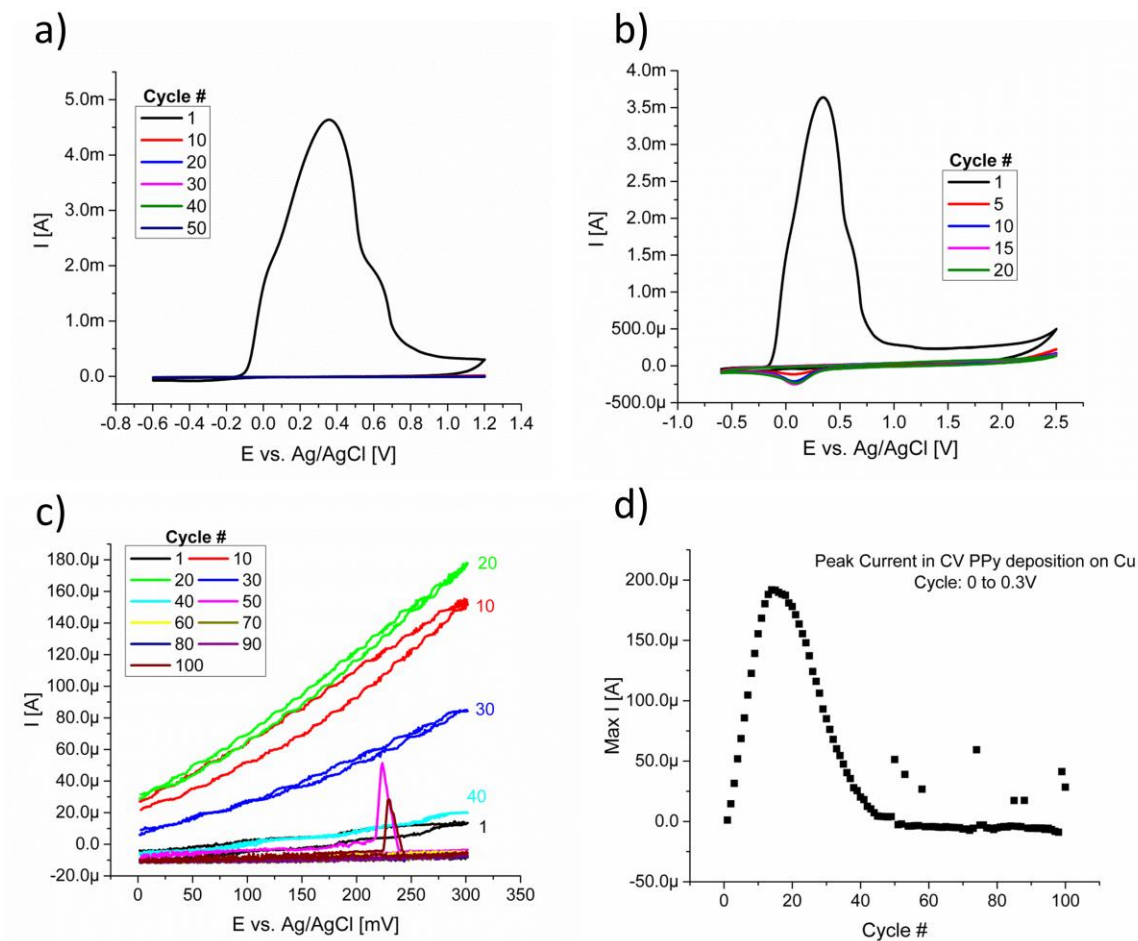


Fig. S7 Attempted deposition of PPy on copper microelectrodes. **(a)** CV results for deposition of PPy on copper with the standard protocol sweeping from -0.6 to 1.2V. **(b)** CV results of deposition of PPy on copper with a longer voltammetry from -0.6 to 2.5 V. **(c)** Short CV deposition avoiding copper reduction, sweeping potential from 0 to 0.3 V vs Ag/AgCl. **(d)** Peak current in the CV deposition process as a function of deposition cycle exhibiting a peak but a fast reduction to negligible current indicating copper dissolution.

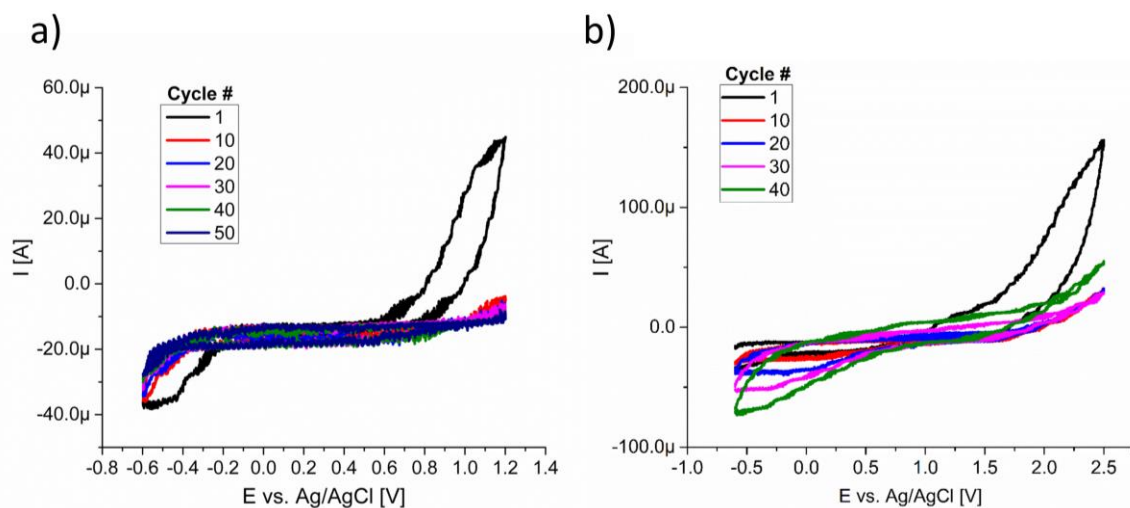


Fig. S8 Attempted deposition of PPy on titanium microelectrodes. **(a)** CV results for deposition of PPy on titanium with the standard protocol sweeping from -0.6 to 1.2V. **(b)** CV results of deposition of PPy on titanium with a longer voltammetry from -0.6 to 2.5 V.

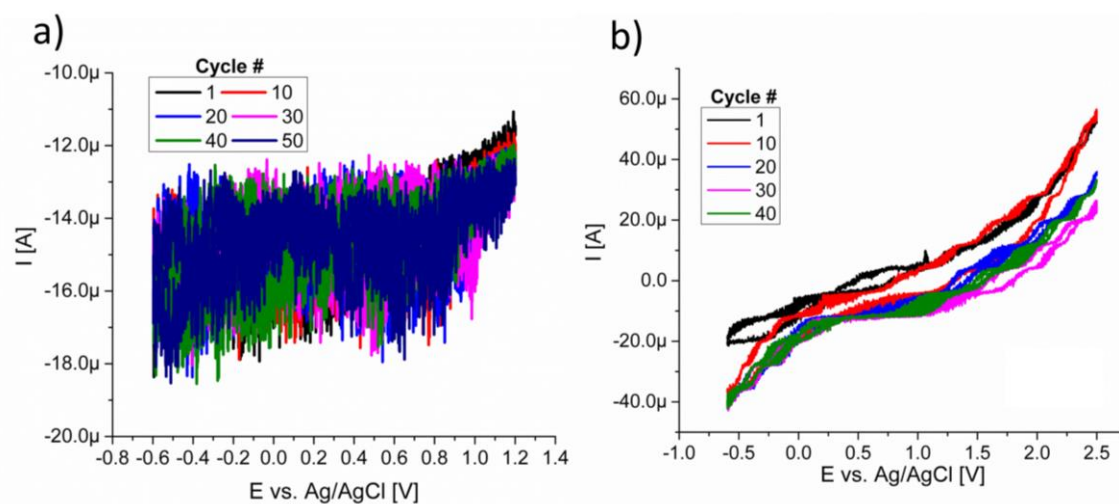


Fig. S9 Attempted deposition of PPy on aluminum microelectrodes. **(a)** CV results for deposition of PPy on aluminum with the standard protocol sweeping from -0.6 to 1.2V. **(b)** CV results of deposition of PPy on aluminum with a longer voltammetry from -0.6 to 2.5 V.

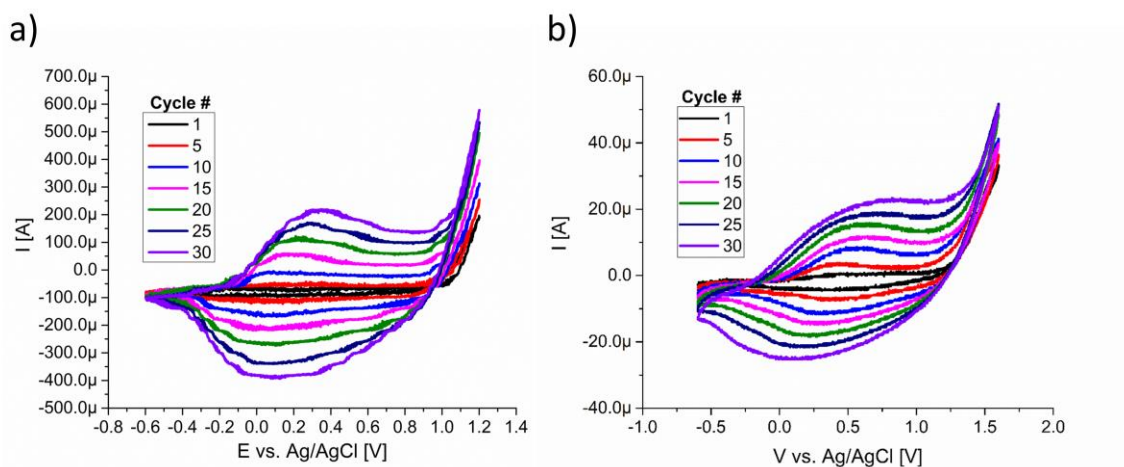


Fig. S10 Results of the CV deposition process on a (a) platinum and (b) nickel microelectrode patterned on an ISFET chip. The peak currents obtained are minor because the electrode area is smaller than in other experiments. However, the shape and evolution of the voltammograms are as expected.

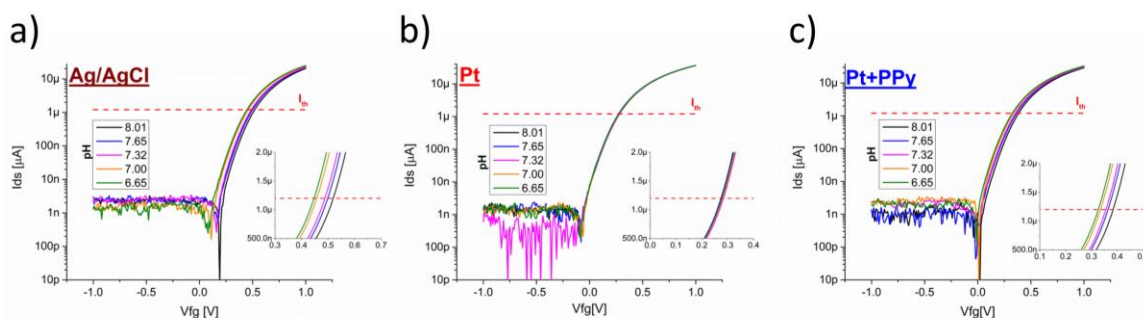


Fig. S11 pH-dependent transfer curves of ISFET biased with different fluid electrodes. The plots show I_d - V_g plots of the ISFET gated with (a) Ag/AgCl, (b) platinum, and (c) platinum + PPy electrodes. The insets zoom in the area of threshold current that is used to extract threshold voltage and surface potential changes.

Supplementary discussion: *Ineffective polypyrrole electrodeposition in semiconductor foundry metals.*

Deposition of the partially oxidized polypyrrole (PPy) film in the microelectrode was not possible with the described cyclic voltammetry deposition protocol in copper, titanium, or aluminum microelectrodes. Given the ubiquitousness of copper for metallization layers in semiconductor foundries, the first deposition assays were performed in copper patterned microelectrodes. The CV process shows that a first cycle reaches high currents and a potential peak that matches the copper reduction potential (Fig. S4a and S4b). However in subsequent cycles there is a negligible current and no deposition of PPy film in the electrode at the end of the process. The curve of the first cycle indicates that copper is being quickly dissolved and without copper on the electrode the deposition is unsuccessful. To prevent dissolution and etch of the copper layer, we attempted to reduce the voltammogram sweep covering only from 0 to 0.3V vs. Ag/AgCl. However, as it is shown in Fig. S4c and S4d, the current also decays to negligible values after initial cycles and the electrode is not coated with the PPy film. Previous reports demonstrated other approaches to deposit PPy on copper utilizing the interaction between a cupric precursor and the polymer monomers¹. Nevertheless those alternatives were not pursued in this study since those additional reagents and steps will complicate the process undermining CMOS compatibility and facile integration.

Deposition on Titanium and Aluminum microelectrodes suffered from low conductivity of metals or the formation of a metal oxide that prevented PPy film polymerization. The cyclic voltammograms of the attempted deposition in titanium are presented in Fig. S5. After an initial cycle with a small peak the following cycles have negligible current. It is possible that in the first cycle the titanium grain boundaries are passivated but the low

conductivity of titanium prevent successful PPy polymerization. Similarly, in aluminum there are only very small currents during deposition (Fig. S6). Quick formation of an alumina layer when the electrodes are exposed to air and during the voltammetry can explain the low conductivities that resulted in unsuccessful polymerization. Similarly to the case of copper, previous publications describe strategies to coat aluminum and titanium electrodes with PPy. For example, Tallman et al., used Tiron® (4,5-dihydroxy-1,3-benzenedisulfonic acid disodium salt) and toluene sulfonic acid sodium salt as the mediators for the deposition process obtaining better coating with Tiron². Also, Giglio et al., reported the use of oxygen depleted electrolytes and mechanical polishing to electrodeposit polypyrrole on titanium and titanium alloys³. Then, deposition on other microelectrodes might be possible by changing the polymerization protocol. However, these approaches went over the scope of this study that targeted to achieve a simple and easily translatable fabrication of an on-chip reference electrode. Further studies that incorporate these techniques for the PPy polymerization may indicate that these protocols could also be used for fabrication of quasi-reference electrodes for ISFET operation, amplifying the range of metals that can be coated with PPy to bias an electrolyte.

References

- 1 Y. Liu, Z. Liu, N. Lu, E. Preiss, S. Poyraz, M. J. Kim and X. Zhang, *Chem. Commun. (Camb)*, 2012, **48**, 2621–3.
- 2 D. E. Tallman, C. Vang, G. G. Wallace and G. P. Bierwagen, *J. Electrochem. Soc.*, 2002, **149**, C173.
- 3 E. De Giglio, M. . Guascito, L. Sabbatini and G. Zambonin, *Biomaterials*, 2001, **22**, 2609–2616.